JACS
JOURNAL OF THE AMERICAN CHEMICAL SOCIETY
Article
pubs.acs.org/JACS

Donor-Dependent Kinetics of Interfacial Proton-Coupled Electron Transfer

Megan N. Jackson and Yogesh Surendranath*

Department of Chemistry, Massachusetts Institute of Technology, Cambridge, Massachusetts 02139, United States

Supporting Information

ABSTRACT: The effect of the proton donor on the kinetics of interfacial concerted proton−electron transfer (CPET) to polycrystalline Au was probed indirectly by studying the rate of hydrogen evolution from trialkylammonium donors with different steric profiles, but the same pK_a. Detailed kinetic studies point to a mechanism for HER catalysis that involves rate-limiting CPET from the proton donor to the electrode surface, allowing this catalytic reaction to serve as a proxy for the rate of interfacial CPET. In acetonitrile electrolyte, triethylammonium ($TEAH^+$) displays up to 20-fold faster CPET kinetics than diisopropylethylammonium ($DIPEAH^+$) at all measured potentials. In aqueous electrolyte, this steric constraint is largely lifted, suggesting a key role for water in mediating interfacial CPET. In acetonitrile, $TEAH^+$ also displays a much larger transfer coefficient (β = 0.7) than $DIPEAH^+$ (β = 0.4), and $TEAH^+$ displays a potential-dependent H/D kinetic isotope effect that is not observed for $DIPEAH^+$. These results demonstrate that proton donor structure strongly impacts the free energy landscape for CPET to extended solid surfaces and highlight the crucial role of the proton donor in the kinetics of electrocatalytic energy conversion reactions.

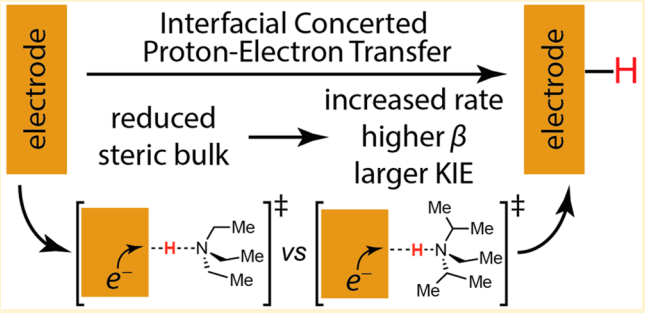

INTRODUCTION

The interconversion of electrical and chemical energy requires the intimate coupling of multiple protons and electrons with small molecules such as H_2O, O_2, and CO_2.[1−3] Energy storage and release reactions involving these small molecules underlie the operation of modern energy storage and utilization devices including electrolyzers, fuel cells, and metal-air batteries. In these devices, the large kinetic barriers to multielectron activation of small molecules are surmounted by heterogeneous catalysts that bind reaction intermediates at surface active sites.[4,5] Despite their central role in virtually all energy storage and release reactions, the mechanistic details of proton−electron coupling at catalyst surfaces remain poorly understood.

A vigorous search for improved energy conversion catalysts has centered upon the twin goals of increasing activity and selectivity, especially in reactions that can give rise to multiple products, such as carbon dioxide reduction and oxygen reduction. For heterogeneous catalysts, this problem is compounded by the fact that the relative adsorption energies of key reactive intermediates typically scale together,[6,7] making it difficult to control reaction selectivity by altering surface structure alone. In biological systems, enzymes are able to control selectivity and efficiency by using proton-shuttling residues in the second coordination sphere of metallo-cofactors to modulate the relative rates of different PCET steps.[8−11] Similarly, in molecular systems, the proton donor has been shown to dictate product selectivity in the case of CO_2 reduction,[12] and the incorporation of proton relays in ligand frameworks has been shown to improve rates and selectivity in molecular electrocatalysts for H_2 evolution,[13,14] O_2 reduction,[15,16] and CO_2 reduction.[17−19] Despite this precedent, in heterogeneous systems, the role of the proton donor has been largely ignored.

The most elementary interfacial PCET reaction is the direct formation of a surface metal−H (M−H) bond. This M−H species is the key intermediate in hydrogen evolution catalysis, making it an ideal platform for studying interfacial PCET kinetics. In molecular hydrogen evolution reaction (HER) catalysts, PCET to form an M−H intermediate is typically believed to proceed through one of two mechanisms (Scheme 1a). In a stepwise "EPT" pathway, equilibrium electron transfer (ET) to the molecular catalyst precedes proton transfer (PT) to the reduced metal center, whereas in a concerted pathway,

Scheme 1. (a) Molecular HER Electrocatalysis May Be Mediated by EPT or CPET Pathways; (b) Heterogeneous HER Electrocatalysis Must Be Mediated by CPET

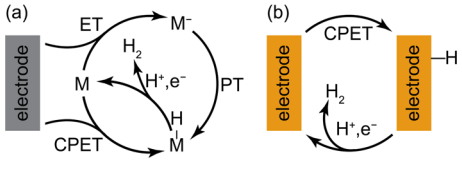

Received: January 6, 2016
Published: February 10, 2016

DOI: 10.1021/jacs.6b00167
J. Am. Chem. Soc. 2016, 138, 3228−3234

the proton and electron transfer simultaneously to the metal center in a concerted proton−electron transfer (CPET) step. Although CPET may possess a high kinetic barrier associated with a formally ternary reaction, the concerted pathway avoids formation of high-energy charged intermediates.[20] In fact, the CPET pathway is always preferred from a thermodynamic standpoint because the intermediate formed after a single PT or ET step is always uphill of the final product, otherwise the charged intermediate would be the final product.[21] It follows that promoting the CPET pathway in a molecular system necessitates an understanding of what makes its kinetic barrier tractable relative to those for the individual PT and ET steps.

Extensive experimental and computational studies have shed light onto the kinetics of these processes. In particular, electrochemical techniques have been heavily utilized in understanding CPET in molecular systems.[20,22−30] Cyclic voltammetry allows for precise control over the applied driving force, and each measurement is a direct probe of ET kinetics. Just as in molecular ET, electrochemical ET kinetics can be described by Marcus theory, in which the rate has an exponential dependence on the thermodynamic driving force, ΔG°, and the net reorganization energy, λ:[31]

$$k_{ET} = Ae^{-(\Delta G^\circ+\lambda)^2/4\lambda RT} \quad (1)$$

PT can be understood in much the same way, with a few caveats.[20−30,32−35] Although PT has been effectively modeled using a nonlinear free energy relation very similar to those employed in Marcus models for ET,[36] PT steps in molecular systems require preorganization of the proton donor and proton acceptor, usually in the form of a hydrogen-bonded complex. This requirement places stringent demands on the structural complementarity of the proton donor and acceptor that are largely nonexistent for electron donor/acceptor pairs. Additionally, PT is slower than ET, and while the Franck−Condon principle allows us to assume no motion in either the reactant or product nuclei over the course of an ET step, the same cannot be said for the PT step. In fact, quite the opposite: the vibrational coupling between the donor and acceptor molecules often determines the probability of PT in a given system.[22−26] Consequently, the molecular structure of the proton donor is a critical determinant of the rate of PCET.[37,38] Indeed, careful optimization of the flexibility, structure and orientation of pendant proton donors has proven critical for the design of highly active molecular electrocatalysts for H_2 evolution,[13,14] O_2 reduction,[15,16] and CO_2 reduction.[17−19]

In contrast to molecular systems, M−H bond formation at a heterogeneous metal surface *must* occur via the concerted pathway (Scheme 1b). Both the stepwise EPT and PET pathways are excluded because the extended band structure in a metal leads to complete delocalization of charge over the entire metal. Thus, it is incorrect to describe an electronic configuration in which charge is localized at any one atom, making it impossible for ET to occur without surface bond formation, and for bond formation to occur without electron transfer from the external circuit. The high density of states in metals makes this true, even for undercoordinated surface sites. Consistent with this expectation, no redox processes are observed in cyclic voltammograms of metal electrodes in the absence of a proton donor or other reducible species. Consequently, heterogeneous M−H bond formation at the surface must proceed via a CPET mechanism and is expected to be highly dependent on the structure of the proton donor. Despite this intuition, there currently exists little understanding of the structural requirements for efficient CPET to an electrode surface, making it difficult to augment the rate of catalytic fuel formation and consumption in a systematic fashion.

In this study, we probe the structural requirements of interfacial CPET by using the rate of HER catalyzed by polycrystalline Au surfaces as a proxy for the rate of CPET to the surface. Au displays a very low H-adsorption energy,[5] so the formation of the Au−H bond is expected to be rate-limiting for HER catalysis. Consistent with this expectation, studies in an acidic, aqueous medium indicate that Au-catalyzed HER proceeds via a rate-limiting one-electron, one-proton step to form a surface-bound H atom.[39,40] An H/D kinetic isotope effect (KIE) of 4.3 has been observed under these conditions, consistent with CPET to form the Au−H intermediate.[41] Thus, Au-catalyzed HER provides an ideal platform for studying the rate of interfacial CPET because the rate of HER on Au *is* the rate of CPET.

Nearly all kinetic studies of HER on Au have been conducted in aqueous acid electrolyte, a medium that presents the surface with the least hindered proton donor, solvated H^+, which sheds little light on the sensitivity of interfacial CPET to the structure of the proton donor. Herein, we examine the effect of proton donor structure on CPET by comparing the rates of HER catalysis on polycrystalline Au using two trialkylammonium proton donors of identical pK_a but drastically different steric profiles. We demonstrate that, in acetonitrile, the structure of the proton donor determines not only the rate of CPET but also the apparent transfer coefficient for the reaction and the magnitude of the H/D kinetic isotope effect. Additionally, the rate of CPET is largely insensitive to proton donor sterics in aqueous media, suggesting the key role of water in mediating interfacial CPET in aqueous electrolytes.

RESULTS

The kinetics of Au-catalyzed hydrogen evolution were investigated using two trialkylammonium cation proton donors, triethylammonium ($TEAH^+$) and diisopropylethylammonium ($DIPEAH^+$). These two acids have the same pK_a (19 in acetonitrile and 11 in water)[42,43] and are constitutionally similar. However, diisopropylethylamine (DIPEA), with a Tolman cone angle of 200°, is significantly more sterically bulky than triethylamine (TEA) with a Tolman cone angle of 150° (see SI for details of the Tolman cone angle calculation for DIPEA).[44]

All electrochemical experiments were conducted using a polycrystalline Au rotating disk working electrode (0.196 cm^2). For studies in acetonitrile, cyclic voltammograms were recorded on stationary electrodes at 20 mV s^{-1} in 100 mM tetrabutylammonium hexafluorophosphate and 20 mM triethylammonium triflate salt (Figure 1). Steady-state data were collected in the presence of excess TBA PF_6 (500 mM) to mitigate migration effects at the electrochemical double layer.[45]

Cyclic voltammograms (CVs) (Figure 1) show an earlier onset of HER for $TEAH^+$ than $DIPEAH^+$ in CH_3CN. Potential vs activation-controlled current density (Tafel) data (Figure 2) were collected galvanostatically for each proton donor by measuring the potential at eight different logarithmically spaced current densities between 51 μA cm^{-2} and 5.1 mA cm^{-2}. Measurements were made in the presence of 25 mM $TEAH^+OTf^-$ or $DIPEAH^+OTf^-$ and 2.5 mM of the corresponding amine. Excess acid was used in all experiments to minimize

DOI: 10.1021/jacs.6b00167
J. Am. Chem. Soc. 2016, 138, 3228−3234

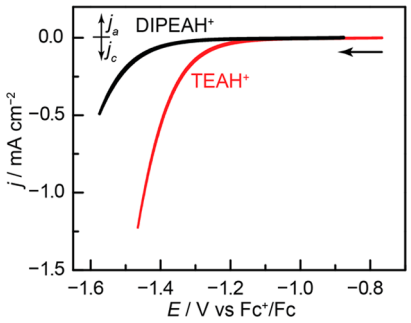

Figure 1. Cyclic voltammograms (20 mV s^{-1}) of polycrystalline Au recorded in acetonitrile containing 0.1 M TBA PF_6, 20 mM $DIPEAH^+OTf^-$ (black) and 20 mM $TEAH^+OTf^-$ (red).

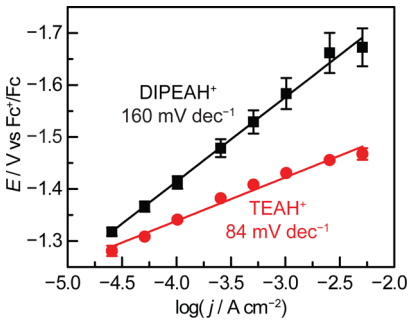

Figure 2. Potential vs activation controlled current density for hydrogen evolution catalysis on polycrystalline Au recorded in acetonitrile containing 0.5 M TBA PF_6, 25 mM $DIPEAH^+OTf^-$ (black) and 25 mM $TEAH^+OTf^-$ (red). Both electrolytes contained 2.5 mM of the corresponding conjugate base. Tafel slopes were 160 and 84 mV dec^{-1}, respectively.

the formation of an association complex between the ammonium and the amine.[46] Electrolyses were conducted at each current density until the potential reached a steady state value. The potentials were corrected for ohmic losses and referenced to ferrocenium/ferrocene (Fc^+/Fc) at the end of each run. The Tafel slopes for HER from $TEAH^+$ and $DIPEAH^+$ were 84 and 160 mV dec^{-1}, respectively, and the HER activity of $TEAH^+$ was greater than that of $DIPEAH^+$ at all measured current densities (Figure 2). The Tafel slopes were similar between forward and reverse sweeps of the current density (Figures S3 and S4), indicating the Tafel behavior was not significantly impacted by transient deactivation of the electrode surface. Additionally, the small error bars in Figure 2 evince the high run-to-run reproducibility of the data under these conditions. Nearly identical current−potential profiles are observed for Au electrodes rotated at 1000 and 2000 rpm (Figures S5 and S6).

The dependence of HER catalytic current density on $TEAH^+$ and $DIPEAH^+$ concentrations was determined by collecting galvanostatic Tafel data across seven current densities between 51 μA cm^{-2} and 5.1 mA cm^{-2} at 10, 20, 50, and 100 mM acid concentrations. Plots of the logarithm of the current density vs the logarithm of the acid concentration were constructed by interpolating the Tafel plots (Figures S7 and S8) at various potentials spanning the data range (Figure 3). The slopes of the resulting linear plots gave reaction orders of ∼0.5 for both $TEAH^+$ and $DIPEAH^+$.

To determine the values of the H/D kinetic isotope effects (KIE) in these systems, current−potential data were collected in deuterated acid ($TEAD^+$ and $DIPEAD^+$) (Figure 4). The

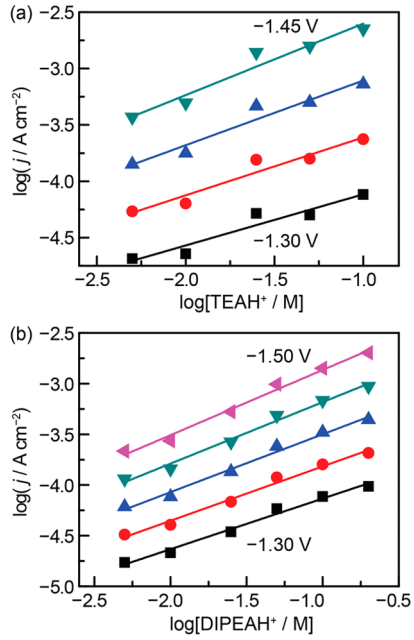

Figure 3. Hydrogen evolution catalytic current density vs concentration of $TEAH^+$ (a) and $DIPEAH^+$ (b). Traces correspond to potentials spaced in 50 mV increments ranging between −1.30 and −1.45 V for $TEAH^+$ and −1.30 and −1.50 V for $DIPEAH^+$. Current densities were recorded on polycrystalline Au in acetonitrile containing 0.5 M TBA PF_6. The slopes range from 0.5 to 0.6 for $TEAH^+$ and from 0.5 to 0.6 in $DIPEAH^+$.

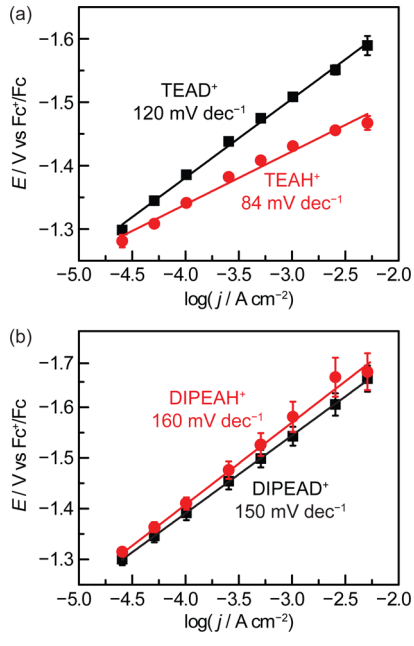

Figure 4. Potential vs activation controlled current density for hydrogen evolution catalysis on polycrystalline Au recorded in acetonitrile containing 0.5 M TBA PF_6, 25 mM $TEAH/D^+OTf^-$ (a) and 25 mM $DIPEAH/D^+OTf^-$ (b). Both electrolytes contained 2.5 mM of the corresponding conjugate base. Tafel slopes were 120, 84, 160, and 150 mV dec^{-1} for $TEAH^+$, $TEAD^+$, $DIPEAH^+$, and $DIPEAD^+$, respectively.

Tafel slope measured for $TEAD^+$ was 120 mV dec^{-1}, which is greater than the 84 mV dec^{-1} Tafel slope observed for $TEAH^+$.

DOI: 10.1021/jacs.6b00167
J. Am. Chem. Soc. 2016, 138, 3228−3234

The Tafel slopes were more similar for $DIPEAH^+$: 150 mV dec^{-1} for $DIPEAD^+$ vs 160 mV dec^{-1} for $DIPEAH^+$.

In aqueous media, Tafel data for HER catalysis with both amine donors were measured over the same current range in 1 M $NaClO_4$, pH 10.7, electrolyte containing 50 mM of either 1:1 TEA:$TEAH^+ClO_4^-$ or DIPEA:$DIPEAH^+ClO_4^-$. Both ammonium acids have an aqueous pK_a of 10.7. Tafel slopes of 200 and 220 mV dec^{-1} are observed for $TEAH^+$ and $DIPEAH^+$, respectively (Figure 5). The Tafel data are largely

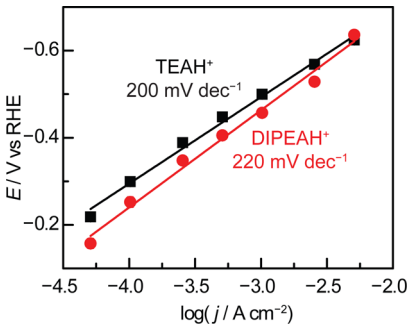

Figure 5. Potential vs activation controlled current density for hydrogen evolution catalysis on polycrystalline Au recorded in aqueous 1 M $NaClO_4$, pH 10.7, electrolyte containing 50 mM TEA/$TEAH^+$ ClO_4 (black) and 50 mM DIPEA/$DIPEAH^+$ ClO_4 (red). Tafel slopes were 200 and 220 mV dec^{-1} for $TEAH^+$ and $DIPEAH^+$, respectively.

invariant with changes in the electrode rotation rate, evincing the absence of transport limitations (Figures S17 and S18). Additionally the data exhibit no significant hysteresis (Figures S15 and S16), indicating that the electrode is not subject to transient deactivation over the time course of the measurement.

DISCUSSION

The Tafel relation between potential and steady state current density (Figure 2), together with studies of reaction order in acid concentration (Figure 3), provide a basis for the mechanistic interpretation of HER from each of these amine donors. The current measured during steady state catalysis is directly proportional to the reaction velocity, provided that the measurement is not subject to mass transport limitations or other experimental artifacts. In our systems, the Tafel behavior was independent of electrode rotation rate (Figures S5 and S6), establishing that the data represent the activation-controlled rate of hydrogen evolution catalyzed by the gold surface. Additionally, the Tafel data were reproducible between independent and sequential measurements and displayed no significant hysteresis (Figures S1, S2, S3, and S4), and CVs recorded after Tafel data collection show no stripping features (Figures S25 and S26), establishing that the electrodes were not subject to transient activation or deactivation over the course of data collection. The measured current densities were also invariant with the strength of the supporting electrolyte (Figure S21), indicating that they were not augmented by artifacts arising from diffuse double layer effects.[47] The lowest potential of Tafel data collection was 0.19 V beyond the thermodynamic potential for H_2 evolution from $TEAH^+$ in CH_3CN,[48] ensuring that HER was effectively irreversible under the conditions of data collection, and that the back reaction (H_2 oxidation to H^+) contributed negligibly to the measured current.

The kinetics of hydrogen evolution on Au electrodes in acetonitrile were strongly dependent on the concentration of the trialkylammonium proton donor. For both $TEAH^+$ and $DIPEAH^+$, we observed a fractional reaction order of ~0.5 for a concentration range that spanned more than 1 order of magnitude (Figure 3). CVs at various concentrations confirmed the 0.5 order (Figures S9–S12). The structure of an electrochemical double layer is complex, so each component of the double layer was investigated independently to determine which species influenced the rate of HER. Although trialkylammonium ions may associate with their corresponding conjugate bases through an H-bond bridge, all data were collected under conditions of excess acid concentration, ensuring that, in spite of any homoconjugation equilibria, a large concentration of unassociated acid was available for proton delivery to the surface. In the presence of excess acid, the Tafel data were independent of the concentration of the conjugate base (Figures S22 and S23), indicating that homoconjugation did not impact the rate of HER catalysis. Additionally, the independence of the catalytic current on the base concentration indicates that physisorption or chemisorption of the base to the surface, if operative, did not influence the rate of HER. The CH_3CN used in these experiments was purified and dried prior to use by passing it through a Glass Contour Solvent Purification System, and the residual water concentration was found to be 7 ppm by Karl Fischer titration. In situ IR spectroscopic studies have shown that water adsorbs to Au and Pt electrodes even at ppm concentrations in CH_3CN, suggesting that water may be adsorbed to the electrode under the conditions of this study.[49−52] However, the addition of 30 ppm water to our electrolyte was found to have no effect on the rate of catalysis, suggesting that water adsorption to the surface, if operative, also does not affect the rate of HER (Figures S27 and S28). As highlighted above, the reaction order in proton donor was insensitive to the concentration of supporting electrolyte (Figure S21), indicating that migration effects due to the interfacial electric field did not influence the data.[45] Taken together, these observations suggest that the fractional reaction order in proton donor is a reflection of the intrinsic kinetics of this reaction. Thus, we write the following empirical rate law:

$$j = k_0[\mathrm{TEAH}^+]^{0.5} e^{\alpha EF/RT} \quad (2)$$

where j is the measured steady state current density, k_0 is a potential-independent rate constant, E is the applied potential, α is the experimental transfer coefficient for the reaction, F is Faraday's constant, R is the gas constant, and T is the temperature.

The experimental rate law is similar in form irrespective of the nature of the proton donor and provides the basis for constructing a mechanistic model for HER under these conditions. On the basis of the calculated adsorption energy of 0.39 eV for H atoms on Au surfaces[5] and the measured thermodynamic potential for HER from $TEAH^+$ in CH_3CN,[48] the thermodynamic potential for the formation of the Au−H bond under our experimental conditions is −1.49 V vs Fc^+/Fc, which is beyond the range of Tafel data collection for $TEAH^+$ (Figure 2). These thermodynamic considerations, along with the absence of H-adsorption waves in cyclic voltammograms (Figure 1), lead us to postulate a catalyst resting state with low surface coverage of adsorbed H.

The Tafel slope provides information about the steps that occur from the resting state up to and including the rate-

DOI: 10.1021/jacs.6b00167
J. Am. Chem. Soc. 2016, 138, 3228−3234

limiting step. We observed Tafel slopes ranging from 84 to 160 mV dec^{-1} in acetonitrile, corresponding to transfer coefficient, α, values ranging from 0.4 to 0.7 (Table 1). These values are

Table 1. Tafel Slope and Transfer Coefficient for Hydrogen Evolution from Each Proton Donor Measured in CH_3CN

donor	Tafel slope (mV dec^{-1})	transfer coefficient (α)
$TEAH^+OTf^-$	84	0.7
$DIPEAH^+OTf^-$	160	0.4
$TEAD^+OTf^-$	120	0.5
$DIPEAD^+OTf^-$	150	0.4

consistent with rate-limiting one-electron transfer from the catalyst resting state,[53] which for HER corresponds to rate-limiting CPET.[54] In situ infrared (IR) spectroscopy indirectly supports a mechanism involving a low population of Au−H and rate-limiting CPET; although Pt−H bonds have been observed in in situ IR studies,[55−57] to our knowledge, surface Au−H bonds have never been observed. Although the reaction order in proton donor is expected to be unity for rate-limiting CPET, fractional orders have been observed in HER electrocatalysis and have been attributed to adsorption phenomena,[58,59] which we do not believe to be operative in this case due to the independence of HER activity on base concentration (Figure S18 and S19). In this case, the fractional order is difficult to explain from experimentally attainable information. It may arise from a nonlinear scaling of the proton donor activity at the interface relative to changes in its bulk concentration, although the precise physical phenomenon leading to an apparent half-order is unknown. We do note that all other sequences would be expected to give rise to reaction orders of 2 (see SI for analysis of possible mechanistic pathways). Together, the data point to the following mechanistic model:

$$\textbf{Step 1}: \text{Au}^* + \text{BH}^+ + \text{e}^- \xrightarrow{k_1} \text{Au-H} + \text{B}$$

$$\textbf{Step 2}: \text{Au-H} + \text{BH}^+ + \text{e}^- \rightarrow \text{H}_2 + \text{B} + \text{Au}^*$$

$$\text{or } 2\text{Au-H} \rightarrow \text{H}_2 + 2\text{Au}^*$$

Au* denotes only the active sites on the surface of a polycrystalline Au electrode; it does not refer to Au sites that are passivated with kinetically inert species or are otherwise catalytically inactive.

For this sequence, the reaction velocity, ν, at steady state can be described by the following rate expression:

$$\nu = 2Fk_1(a_{\text{BH}^+})\theta_{\text{Au}^*}e^{\beta EF/RT} \quad (3)$$

where k_1 denotes the potential-independent rate constant for the CPET step, $a_{\text{BH}+}$ is the activity of proton donor in the electrochemical double layer, and θ_{Au^*} is the surface concentration of Au active sites (Γ_{Au^*}, in mol/cm^2) divided by the total surface concentration of Au atoms (Γ_{max}). The exponential term in eq 3 describes the relationship between applied potential and reaction rate for a one-electron irreversible charge transfer step in which β is the symmetry factor. Given the low coverage of Au−H species, θ_{Au^*} can be taken as a constant close to unity. Under these assumptions, the rate expression is similar in form to the empirical rate law, apart from a suppressed reaction order in proton, and the empirical transfer coefficient, α, equals the symmetry factor for an irreversible one-electron transfer step, β.

Since the kinetic behavior of both proton donors is most consistent with rate-limiting CPET to the electrode for HER, we can directly compare the catalytic activity of the two donors to determine the effect of steric profile on a substrate's ability to donate a proton to an electrochemical interface. $TEAH^+$ exhibited higher HER catalytic activity than $DIPEAH^+$ at all measured potentials. This result is readily visualized in the CVs (Figure 1). At the lowest potential probed, −1.32 V vs Fc^+/Fc, the activities of the two donors differed by a factor of 2.5, whereas at −1.47 V vs Fc^+/Fc, the rate of HER from $TEAH^+$ was 20-fold greater than the rate of HER from $DIPEAH^+$. Since both molecules have pK_a values of 19 in acetonitrile, this activity difference is likely due to a difference in kinetic barriers rather than a difference in driving force. This observation is consistent with previous studies (and our chemical intuition) that have shown that the preexponential term is correlated to the distance between an ammonium proton donor and acceptor.[60] Put simply, the less sterically encumbered proton donor delivers protons to the electrode surface more rapidly.

Interestingly, the two proton donors gave rise to dramatically different Tafel slopes, leading to a potential-dependent difference in HER activities. This proton donor-dependent Tafel behavior is reflective of the strong dependence of β on the structure of the proton donor. However, the observed range of β values is not readily explained by current theories of interfacial charge transfer. For an outer-sphere electron transfer, a Marcus-type model can be applied to derive the following analytic expression for the symmetry factor:[47]

$$\beta = -\frac{1}{F}\frac{\delta}{\delta\eta}\frac{(\eta^2F^2 - 2\eta F\lambda + \lambda^2)}{4\lambda} = \frac{1}{2} - \frac{\eta F}{2\lambda} \quad (4)$$

where λ is the electron transfer reorganizational energy, η is the overpotential for the rate-limiting CPET step, and the other symbols adopt their normal meanings. If η is small relative to λ, β limits to 0.5, so the expected Tafel slopes are 120 mV dec^{-1}. Although Marcus theory was originally developed to describe outer-sphere electron transfer, empirically, HER with rate-limiting inner-sphere one-electron transfer steps also tends to exhibit symmetry factors close to 0.5 in aqueous media.[54]

Previously, when inner-sphere electron transfer coefficients have deviated from 0.5, it has been attributed to factors unrelated to λ. They are most often attributed to variations in charge distribution in the double layer.[61] While this factor undoubtedly plays a role in determining the rate of interfacial electron transfer, in our experimental conditions, the double layer consisted primarily of TBA PF_6 in both cases. In the case of ET from an Os aquo complex tethered to a Au electrode, computations suggested that the deviation from 0.5 for β was due to a potential-dependence in the equilibrium distance between the molecule and the electrode.[22,62] We rule out this phenomenon as the sole explanation for the difference in β observed here because it is unlikely that two similar trialkylamines would have opposite potential-dependent equilibrium distances from the electrode. Instead, we postulate that the difference in β arises from differences in the structure of the proton donor itself.

Our experiments allow us to explicitly examine the dependence of β on proton donor structure. Previous studies of driving force/rate relationships for proton transfers, hydride transfers,[63] hydrogen atom transfers,[64] and other PCET reactions[21,65] typically apply the Marcus cross relation to a series of donor−acceptor pairs rather than a direct measure-

DOI: 10.1021/jacs.6b00167
J. Am. Chem. Soc. 2016, 138, 3228−3234

ment of driving force−rate scaling for any individual ion donor. Indeed, for all of these reactions, changes in the driving force necessitate changes in the structure of the donor or acceptor, making this method largely insensitive to small changes in the CPET transfer coefficient between different molecules. Whereas electrochemical studies of CPET in molecular systems allow for independent modulation of the ET driving force, changes in driving force typically lead to a transition from concerted to stepwise PCET, making it difficult to extract a transfer coefficient for the former. Indeed, this experimental challenge has led to the widespread assumption that β = 0.5 when modeling experimental voltammetry data for outer sphere CPET systems.[66] Here, we observe large deviations from β = 0.5 based on the structure of the donor, suggesting that this assumption may not apply in all cases and that a simple Marcusian approximation of the kinetics of inner sphere CPET processes is insufficient.

Importantly, β is dependent not only on the structure of the proton donor but also on the nature of the atom being donated to the electrode. In the case of $TEAH^+$, when the H atom was replaced with a D atom, we observed a dramatic change in Tafel slope from 84 to 120 mV dec^{-1}, corresponding to a change in β from 0.7 to 0.5. The differing Tafel slopes led to a potential-dependent kinetic isotope effect ranging from 4.9 to 19 (Figure 4). In contrast, when $DIPEAH^+$ was the proton donor, we observed no significant difference between HER activity and DER activity, suggesting a KIE of <2. PCET processes are known to display H/D KIE ranging from <2 to >450, and our current level of understanding makes it difficult to predict which systems will exhibit large KIE values and which will not.[25,67] However, studies typically evaluate KIE at a single driving force, and the few that have examined driving-force dependent KIE also observe a positive correlation between the two.[60] Computed KIE values for molecular systems rely primarily on proton potential energy surfaces and probability distribution functions, and predict a negligible difference in solvent reorganization energy for H and D;[24] however, KIE values for interfacial CPET have not been computed. Our measurements suggest that the magnitude of interfacial KIE values are also strongly dependent on the reaction free energy.

Notably, the donor dependence of β is also strongly influenced by the electrolyte environment. In aqueous electrolyte, in which water can act as a proton donor, there is a negligible difference in HER activity and Tafel slope between $TEAH^+$- and $DIPEAH^+$-buffered solutions across all measured potentials, suggesting that the ammonium salt no longer interacts directly with the electrode to form the Au−H bond. Instead, it appears that H_2O mediates the transfer of protons to the Au surface, analogous to what is observed in molecular systems in which water has been shown to play an essential role in promoting CPET pathways.[68]

CONCLUSION

We have demonstrated that the rate of CPET to a Au electrode in acetonitrile is strongly dependent on the molecular structure of the proton donor. The less bulky donor, $TEAH^+$, was found to have higher HER activity at all measured potentials than the bulkier $DIPEAH^+$. Additionally, both the steric profile of the donor and the nature of the atom being donated (H or D) were found to affect the electron transfer coefficient, β. These factors led to donor-dependent Tafel slopes and driving force-dependent H/D kinetic isotope effects. In contrast, in aqueous media, we observed no significant difference in HER activity or transfer coefficient between the two ammonium proton donors, suggesting that H_2O effectively mediates interfacial CPET and relaxes the structural requirements for facile PCET to electrode surfaces.

The significance of these results is two-fold. The strong dependence of β on the molecular structure and identity of the proton donor suggests that there remains a lack of understanding of the free-energy landscape for interfacial ion transfer processes. Additionally, the strong dependence of interfacial CPET on proton donor structure suggests that suitably designed acids can be used to direct the selectivity of interfacial reactions, particularly in aprotic electrolytes. Likewise, the results suggest that water's unique role as a promiscuous proton donor[68] must be managed in order to direct multielectron reaction selectivity in aqueous electrolytes.

ASSOCIATED CONTENT

Supporting Information

The Supporting Information is available free of charge on the ACS Publications website at DOI: 10.1021/jacs.6b00167.

Full experimental details, additional Tafel data, and raw reaction order data. (PDF)

AUTHOR INFORMATION

Corresponding Author

*yogi@mit.edu

Notes

The authors declare no competing financial interest.

ACKNOWLEDGMENTS

We gratefully acknowledge Kwabena Bediako for fruitful discussions. The research was supported by the Air Force Office of Scientific Research under award FA9550-15-1-0135 and by the MIT Department of Chemistry through junior faculty funds for Y.S. M.N.J. is supported by the Department of Defense (DoD) through the National Defense Science & Engineering Graduate Fellowship (NDSEG) Program.

REFERENCES

(1) Saveant, J.-M. *Elements of Molecular and Biomolecular Electrochemistry: An Electrochemical Approach to Electron Transfer Chemistry*; John Wiley & Sons, Inc.: Hoboken, NJ, 2006.

(2) Weinberg, D. R.; Gagliardi, C. J.; Hull, J. F.; Murphy, C. F.; Kent, C.; Westlake, B. C.; Paul, A.; Ess, D. H.; McCafferty, D. G.; Meyer, T. J. *Chem. Rev.* **2012**, *112*, 4016.

(3) Nocera, D. G. *Inorg. Chem.* **2009**, *48*, 10001.

(4) Quaino, P.; Santos, E.; Soldano, G.; Schmickler, W. *Adv. Phys. Chem.* **2011**, *2011*, 1.

(5) Norskov, J. K.; Bligaard, T.; Logadottir, A.; Kitchin, J. R.; Chen, J. G.; Pandelov, S.; Stimming, U. *J. Electrochem. Soc.* **2005**, *152*, J23.

(6) Abild-Pedersen, F.; Greeley, J.; Studt, F.; Rossmeisl, J.; Munter, T. R.; Moses, P. G.; Skúlason, E.; Bligaard, T.; Nørskov, J. K. *Phys. Rev. Lett.* **2007**, *99*, 4.

(7) Jones, G.; Bligaard, T.; Abild-Pedersen, F.; Nørskov, J. K. *J. Phys.: Condens. Matter* **2008**, *20*, 064239.

(8) Reece, S. Y.; Nocera, D. G. *Annu. Rev. Biochem.* **2009**, *78*, 673.

(9) Kaila, V. R. I.; Verkhovsky, M. I.; Wikström, M. *Chem. Rev.* **2010**, *110*, 7062.

(10) Siegbahn, P. E. M.; Blomberg, M. R. a. *Chem. Rev.* **2010**, *110*, 7040.

(11) Glover, S. D.; Jorge, C.; Liang, L.; Valentine, K. G.; Hammarström, L.; Tommos, C. *J. Am. Chem. Soc.* **2014**, *136*, 14039.

(12) Bhugun, I.; Lexa, D.; Saveant, J.-M. *J. Am. Chem. Soc.* **1994**, *116*, 5015.

DOI: 10.1021/jacs.6b00167
J. Am. Chem. Soc. 2016, 138, 3228−3234

(13) Rakowski DuBois, M.; DuBois, D. L. *Chem. Soc. Rev.* **2009**, *38*, 62.
(14) Roubelakis, M. M.; Bediako, D. K.; Dogutan, D. K.; Nocera, D. G. *Energy Environ. Sci.* **2012**, *5*, 7737.
(15) Carver, C. T.; Matson, B. D.; Mayer, J. M. *J. Am. Chem. Soc.* **2012**, *134*, 5444.
(16) Rosenthal, J.; Nocera, D. G. *Acc. Chem. Res.* **2007**, *40*, 543.
(17) Costentin, C.; Drouet, S.; Robert, M.; Savéant, J.-M. *Science* **2012**, *338*, 90.
(18) Wilson, A. D.; Fraze, K.; Twamley, B.; Miller, S. M.; DuBois, D. L.; DuBois, M. R. *J. Am. Chem. Soc.* **2008**, *130*, 1061.
(19) Rakowski DuBois, M.; DuBois, D. L. *Acc. Chem. Res.* **2009**, *42*, 1974.
(20) Bonin, J.; Costentin, C.; Robert, M.; Routier, M.; Savéant, J. M. *J. Am. Chem. Soc.* **2013**, *135*, 14359.
(21) Mayer, J. M. *Annu. Rev. Phys. Chem.* **2004**, *55*, 363.
(22) Ludlow, M. K.; Soudackov, A. V.; Hammes-Schiffer, S. *J. Am. Chem. Soc.* **2010**, *132*, 1234.
(23) Venkataraman, C.; Soudackov, A. V.; Hammes-schiffer, S. *J. Phys. Chem. C* **2008**, *112*, 12386.
(24) Auer, B.; Fernandez, L. E.; Hammes-Schiffer, S. *J. Am. Chem. Soc.* **2011**, *133*, 8282.
(25) Hammes-Schiffer, S.; Iordanova, N. *Biochim. Biophys. Acta, Bioenerg.* **2004**, *1655*, 29.
(26) Navrotskaya, I.; Hammes-Schiffer, S. *J. Chem. Phys.* **2009**, *131*, 024112.
(27) Navrotskaya, I.; Soudackov, A. V.; Hammes-Schiffer, S. *J. Chem. Phys.* **2008**, *128*, 244712.
(28) Costentin, C.; Robert, M.; Savéant, J.-M.; Teillout, A.-L. *Proc. Natl. Acad. Sci. U. S. A.* **2009**, *106*, 11829.
(29) Costentin, C.; Robert, M.; Savéant, J.-M. *Chem. Soc. Rev.* **2013**, *42*, 2423.
(30) Savéant, J.-M. *Energy Environ. Sci.* **2012**, *5*, 7718.
(31) Marcus, R. *Annu. Rev. Phys. Chem.* **1964**, *15*, 155−196.
(32) Bell, R. P. *Proton in Chemistry*, 2nd ed.; Cornell University Press: Ithaca, NY, 1973.
(33) Kresge, A. *Acc. Chem. Res.* **1975**, *8*, 354.
(34) Guthrie, J. P. *J. Am. Chem. Soc.* **1996**, *118*, 12878.
(35) Tanko, J. M.; Friedline, R.; Suleman, N. K.; Castagnoli, N. J. *J. Am. Chem. Soc.* **2001**, *123*, 5808.
(36) Kiefer, P. M.; Hynes, J. T. *J. Phys. Chem. A* **2002**, *106*, 1834.
(37) Costentin, C.; Robert, M.; Savéant, J. M.; Tard, C. *Angew. Chem., Int. Ed.* **2010**, *49*, 3803.
(38) Bonin, J.; Costentin, C.; Robert, M.; Savéant, J. M.; Tard, C. *Acc. Chem. Res.* **2012**, *45*, 372.
(39) Eberhardt, D.; Santos, E.; Schmickler, W. J. *Electroanal. Chem.* **1999**, *461*, 76.
(40) Doubova, L. M.; Trasatti, S. J. *Electroanal. Chem.* **1999**, *467*, 164.
(41) Conway, B. E. *Proc. R. Soc. London, Ser. A* **1960**, *256*, 128.
(42) Kaljurand, I.; Kütt, A.; Sooväli, L.; Rodima, T.; Mäemets, V.; Leito, I.; Koppel, I. *J. Org. Chem.* **2005**, *70*, 1019.
(43) Perrin, D. D. *Dissociation Constants of Organic Bases in Aqueous Solution*; Butterworths: London, 1965.
(44) Bilbrey, J. a.; Kazez, A. H.; Locklin, J.; Allen, W. D. *J. Comput. Chem.* **2013**, *34*, 1189.
(45) Gileadi, E. *Physical Electrochemistry, Fundamentals, Techniques and Applications*; Wiley-VCH: Weinheim, 2011.
(46) Izutsu, K. *Acid-Base Dissociation Constants in Dipolar Aprotic Solvents*; Blackwell Scientific: Oxford, 1990.
(47) Bard, A. J.; Faulkner, L. R. *Electrochemical Methods Fundimentals and Applications*, 2nd ed.; John Wiley & Sons, Inc.: New York, 2001.
(48) Roberts, J. a S.; Bullock, R. M. *Inorg. Chem.* **2013**, *52*, 3823.
(49) Staszak-Jirkovsky, J.; Subbaraman, R.; Strmcnik, D.; Harrison, K. L.; Diesendruck, C. E.; Assary, R.; Frank, O.; Wiberg, G. K. H.; Genorio, B.; Connell, J. G.; Lopes, P. P.; Stamenkovic, V. R.; Curtiss, L.; Moore, S.; Zavadil, K. R.; Markovic, N. M. *ACS Catal.* **2015**, *5*, 6600.
(50) Suarez-Herrera, M. F.; Costa-Figueiredo, M.; Feliu, J. M. *Langmuir* **2012**, *28*, 5286.
(51) Ledezma-Yanez, I.; Díaz-Morales, O.; Figueiredo, M. C.; Koper, M. T. M. *ChemElectroChem* **2015**, *2*, 1612.
(52) Rudnev, A. V.; Zhumaev, U. E.; Kuzume, A.; Vesztergom, S.; Furrer, J.; Broekmann, P.; Wandlowski, T. *Electrochim. Acta* **2016**, *189*, 38.
(53) Santos, E.; Lundin, A.; Pötting, K.; Quaino, P.; Schmickler, W. *Phys. Rev. B: Condens. Matter Mater. Phys.* **2009**, *79*, 1.
(54) Pentland, N.; Bockris, J. O.; Sheldon, E. *J. Electrochem. Soc.* **1957**, *104*, 182.
(55) Kunimatsu, K.; Senzaki, T.; Samjeské, G.; Tsushima, M.; Osawa, M. *Electrochim. Acta* **2007**, *52*, 5715.
(56) Kunimatsu, K.; Senzaki, T.; Tsushima, M.; Osawa, M. *Chem. Phys. Lett.* **2005**, *401*, 451.
(57) Kunimatsu, K.; Uchida, H.; Osawa, M.; Watanabe, M. *J. Electroanal. Chem.* **2006**, *587*, 299.
(58) Ohmori, T.; Enyo, M. *Electrochim. Acta* **1992**, *37*, 2021.
(59) Sasaki, T.; Matsuka, A. *J. Res. Inst. Catal. Hokkaido Univ.* **1981**, *29*, 113.
(60) Markle, T. F.; Rhile, I. J.; Mayer, J. M. *J. Am. Chem. Soc.* **2011**, *133*, 17341.
(61) Schmickler, W.; Santos, E. *Interfacial Electrochemistry* **2010**, DOI: 10.1007/978-3-642-04937-8.
(62) Madhiri, N.; Finklea, H. O. *Langmuir* **2006**, *22*, 10643.
(63) Lee, I. S. H.; Chow, K. H.; Kreevoy, M. M. *J. Am. Chem. Soc.* **2002**, *124*, 7755.
(64) Warren, J. J.; Mayer, J. M. *Proc. Natl. Acad. Sci. U. S. A.* **2009**, *107*, 5282.
(65) Hammes-Schiffer, S.; Soudackov, A. V. *J. Phys. Chem. B* **2008**, *112*, 14108.
(66) Costentin, C.; Drouet, S.; Robert, M.; Savéant, J. M. *J. Am. Chem. Soc.* **2012**, *134*, 11235.
(67) Huynh, M. H. V; Meyer, T. *Proc. Natl. Acad. Sci. U. S. A.* **2004**, *101*, 13138.
(68) Bonin, J.; Costentin, C.; Louault, C.; Robert, M.; Savéant, J. M. *J. Am. Chem. Soc.* **2011**, *133*, 6668.

DOI: 10.1021/jacs.6b00167
J. Am. Chem. Soc. 2016, 138, 3228−3234